



ORIGINAL ARTICLE

Potential of nano crystalline calcium hydroxyapatite for Tin(II) removal from aqueous solutions: Equilibria and kinetic processes



Davod Ghahremani ^a, Iman Mobasherpour ^{b,*}, Esmail Salahi ^b, Mohsen Ebrahimi ^b, Sahebali Manafi ^c, Leila Keramatpour ^d

^a Department of Engineering, Islamic Azad University, Maybod Branch, Maybod, P.O. Box 89516/175, Iran

^b Ceramics Department, Materials and Energy Research Center, Karaj, P.O. Box 31787-316, Iran

^c Department of Ceramics, Islamic Azad University, Shahrood Branch, Shahrood, Iran

^d Islamic Azad University, Science and Research Branch, Tehran, Iran

Received 3 April 2012; accepted 3 October 2012

Available online 17 October 2012

KEYWORDS

Adsorption;
Nano crystalline hydroxyapatite;
Sn²⁺ ion;
Isotherms;
Thermodynamics;
Kinetic

Abstract The potential of the synthesized nano hydroxyapatite to remove Sn²⁺ from aqueous solutions was investigated in a batch reactor under different experimental conditions. The study also investigates the effects of process parameters such as initial concentration of Sn²⁺ ions, temperature, and adsorbent mass. Various thermodynamic parameters, such as ΔG° , ΔH° and ΔS° have been calculated. The thermodynamics of an Sn²⁺ ion onto nano HAp system indicates a spontaneous and endothermic nature of the process. Tin uptake was quantitatively evaluated using the Langmuir, Freundlich and Dubinin–Kaganer–Radushkevich models. The adsorption data follow the adsorption equilibrium described well by the Langmuir isotherm model with maximum adsorption capacity of 2500 mg/g of Sn²⁺ ions on nano HAp. Using the second-order kinetic constants, the activation energy of adsorption (E_a) was determined as 4.125 kJ mol⁻¹ according to the Arrhenius equation.

© 2013 Production and hosting by Elsevier B.V. on behalf of King Saud University. This is an open access article under the CC BY-NC-ND license (<http://creativecommons.org/licenses/by-nc-nd/3.0/>).

1. Introduction

Over the past few decades, rapid industrialization has led to a tremendous increase in the use of heavy metals, which has inevitably resulted in an increased flux of metallic substances in the aquatic environment. Tin is one of the toxic metals found in most wastewaters. Many industries produce large quantities of waste streams containing low concentrations of tin, along with other metals from processes such as tin electroplating, aluminum anodizing, printed circuit board manufacturing, and metal pickling. Recycling metals from such

* Corresponding author. Tel.: +98 (261)6204131; fax: +98 2616201888.

E-mail addresses: davod.ghahremani@gmail.com (D. Ghahremani), Iman.Mobasherpour@gmail.com, I_Mobasherpour@merc.ac.ir (I. Mobasherpour), kesalahi@yahoo.com (E. Salahi), ebrahimi186@yahoo.com (M. Ebrahimi).

Peer review under responsibility of King Saud University.



Production and hosting by Elsevier

solutions is attractive for environmental reasons and for the value of metals (Wasewar et al., 2009).

A level of tin (250 mg/kg) in canned food is generally accepted as a maximum tolerance level for humans. If a large amount of tin in canned food is taken daily over a long period, acute effects such as stomachache, anemia, and liver and kidney problems occur. The Occupational Safety and Health Administration (OSHA) has designated a workplace exposure limit of 0.1 mg/m^3 for organic tin compounds, and 2 mg/m^3 for inorganic tin compounds, except oxide. There are various treatment processes for the removal and/or recovery of heavy metal ions, including precipitation, oxidation, ultrafiltration, electrodiagnosis, solvent extraction, ion exchange, adsorption, etc. (Aksu and Tunc, 2005). For high strength and low volumes of wastewater, heavy metal removal by adsorption is a good proposition.

Hydroxyapatite is an ideal material for long-term containment of contaminants because of its high sorption capacity for actinides and heavy metals, low water solubility, high stability under reducing and oxidizing conditions, availability, and low cost (Krestou et al., 2004). It was used in stabilization of a wide variety of metals (e.g., Cr, Co, Cu, Cd, Zn, Ni, Pu, Pb, As, Sb, U, and V) by many investigators (Chen et al., 1997; Czerniczyniec et al., 2003; Vega et al., 1999; Reichert and Binner, 1996; Leyva et al., 2001; Fuller et al., 2002; McGrellis et al., 2001; Mobasherpour et al., 2011). They reported the sorption to take place through ionic exchange reaction, surface complexation with phosphate, calcium and hydroxyl groups and/or co-precipitation of new partially soluble phases.

Calcium hydroxyapatite (CaHAp), $\text{Ca}_{10}(\text{PO}_4)_6(\text{OH})_2$, is used for the removal of heavy metals from contaminated soils, wastewater and fly ashes (Laperche et al., 1996; Ma et al., 1993; Ma et al., 1994; Mavropoulos, 2002; Nzihou and Sharrock, 2002; Takeuchi and Arai, 1990). Calcium hydroxyapatite (CaHAp) is a principal component of animal hard tissues and has been of interest in industrial and medical fields. Its synthetic particles find many applications in bioceramics, chromatographic adsorbents to separate protein and enzyme, catalysts for dehydration and dehydrogenation of alcohols, methane oxidation, and powders for artificial teeth and bones paste germicides (Elliott, 1994). These properties relate to various surface characteristics of HAp, e.g., surface functional groups, acidity and basicity, surface charge, hydrophilicity, and porosity. It has been found that HAp surface possesses 2.6 groups nm^{-2} of P-OH groups acting as sorption sites (Tanaka et al., 2005). The sorption properties of HAp are of great importance for both environmental processes and industrial purposes.

The objective of this study was to investigate the possible use of nano crystalline hydroxyapatite as an alternative adsorbent material for the removal of Sn^{2+} ions from aqueous solutions. The Langmuir, Freundlich and D-K-R models were used to fit the equilibrium isotherm. The dynamic behavior of the adsorption was investigated on the effect of initial metal ion concentration, temperature, and adsorbent mass of solution. The thermodynamic parameters were also evaluated from the adsorption measurements.

2. Material and methods

2.1. Preparation of nano crystalline hydroxyapatite sorbents

All chemicals used in this work were of analytical grade and the aqueous solutions were prepared using double distilled

water. Nanocrystalline hydroxyapatite compounds were prepared by a solution-precipitation method (Mobasherpour et al., 2007) using $(\text{NH}_4)_2\text{HPO}_4$ (Merck No. 1205) and $\text{Ca}(\text{NO}_3)_2 \cdot 4\text{H}_2\text{O}$ (Analar No. 10305) as starting materials and ammonia solution as agents for pH adjustment. A suspension of $\text{Ca}(\text{NO}_3)_2 \cdot 4\text{H}_2\text{O}$ was vigorously stirred and its temperature was maintained at 25°C . A solution of $(\text{NH}_4)_2\text{HPO}_4$ was slowly added dropwise to the $\text{Ca}(\text{NO}_3)_2 \cdot 4\text{H}_2\text{O}$ solution. In all experiments the pH of $\text{Ca}(\text{NO}_3)_2 \cdot 4\text{H}_2\text{O}$ solution by adding ammonia solution was 11. The precipitate HAp was removed from the solution by the centrifuge method at a rotation speed of 3000 rpm. The resulting powder was dried at 100°C . The particles thus synthesized were characterized by the following methods. Transmission electron microscopy (TEM) was used to characterize the synthesized particles of HAp. For this purpose, particles were deposited onto Cu grids, which support a "holey" carbon film. The particles were deposited onto the support grids by deposition from a dilute suspension in acetone or ethanol. The crystalline shapes and sizes were characterized by diffraction (amplitude) contrast and, for crystalline materials, by high resolution (phase contrast) imaging. The specific surface area was determined from N_2 adsorption isotherm by the BET method using a Micromeritics surface area analyzer model ASAP 2010. The concentrations of Ca^{2+} and PO_4^{3-} in the synthesized particles were determined by inductively coupled plasma atomic emission spectrometer (ICP-AES) by first dissolving the particles in HCl solution. The Fourier transform infrared spectra (FT-IR) of nano hydroxyapatite were recorded using a Perkin-Elmer 2000 FTIR spectrometer calibrated with a deuterated triglycine sulfate (DTGS) detector covering the frequency range of $500\text{--}4000 \text{ cm}^{-1}$. The sample cell was purged with nitrogen gas throughout data collection to exclude carbon dioxide and water vapor. Ten milligrams of the dried samples was dispersed in 200 mg of spectroscopic grade KBr to record the spectra.

The crystal phase was identified by powder X-ray diffraction (XRD) using Siemens (30 kV and 25 mA) X-ray diffractometer with Cu K_α radiation ($\lambda = 1.5404 \text{ \AA}$) and XPERT software.

2.2. Sorption study

All sorption experiments were carried out without any pre equilibrium processes that were imposed during the performance of any experiments. In order to determine the sorption capacity of nano HAp for Sn^{2+} cations, as well as the influence of the initial concentration of Sn^{2+} ion, adsorbent dosage and temperature, sorption experiments were performed by the batch equilibration technique.

Aqueous solutions containing Sn^{2+} ions of concentration (80, 100, 120 and 140 mg/L) were prepared from Sn^{2+} chloride ($\text{SnCl}_2 \cdot 2\text{H}_2\text{O}$, Merck No. 7815). 0.01 g of nano HAp was introduced in a stirred tank reactor containing 500 mL of the prepared solution. The stirring speed of the agitator was 300 rpm. The temperature of the suspension was maintained at $25 \pm 1^\circ\text{C}$. The initial pH of the solution was adjusted to the value 6.5 by adding NH_3 and HCl. Samples were taken after mixing the adsorbent and Sn^{2+} ion bearing solution at pre determined time intervals (5, 10, 20, 30, 60, and 120 min) for the measurement of residual metal ion concentration in

the solution and to ensure equilibrium was reached. After any specified time the sorbents were separated from the solution by centrifuge and filtration through the filter paper (Whatman grade6). The exact concentration of metal ions was determined by AAS (GBC 932 Plus atomic absorption spectrophotometer). All experiments were carried out twice. The mass balance of tin is given by:

$$mq = V(C_0 - C) \quad (1)$$

where m , q , V , C_0 , and C are the mass of nano-HAp (g), amount of tin removed by unit weight of HAp (Uptake capacity: mg Sn/g HAp), volume of tin solution (L), initial tin concentration in the solution (mg Sn/L), and the concentration of tin at the time t of adsorption (mg Sn/L). After 120 min, C and q will reach equilibrium values C_e and q_e .

The percent removal (%) was calculated using the following equations:

$$\% \text{Removal} = \frac{(c_0 - c_t)}{c_0} \times 100 \quad (2)$$

where C_0 and C_t are the concentrations of the metal ion in initial and final solutions (after 120 min).

3. Results and discussion

3.1. Characteristics of adsorbent

TEM micrograph of the HAp powders after drying is seen in Fig. 1a. The microstructure of the HAp crystalline after drying is observed to be almost like needle shape, with size in the range of 20–30 nm. The crystal structure analysis of HAp particles was performed, using X-ray diffraction, and the obtained diffractograms are represented in Fig. 1b. The produced reflection patterns match the ICDD standards (JCPDS) for HAp. The patterns show only the peaks characteristic of the synthesized HAp with no obvious evidence on the presence of other additional phases. The broad patterns around (211) and (002) indicate that the crystallites are very tiny in nature with much atomic oscillations. The sample was indexed in the hexagonal system with space group $P6_3/m$ and Calcium Phosphate Hydroxide ICSD name (Ref. Code.01-074-0565 in XPERT software). The unit cell parameters of nano Hydroxyapatite synthesized were $a = b = 0.9424$ nm and $c = 0.6879$ nm. The analysis of the HAp sample has confirmed a low-crystalline product, with the specific surface area of 94.9 m²/g. The Ca/P molar ratio was found to be 1.65 ± 0.05 instead of 1.67 that represents the characteristic stoichiometric ratio. This cation deficiency is common for the sample obtained by the wet method.

The structure of the powder was analyzed using FT-IR spectroscopy after drying at 100 °C, as shown in Fig. 2. In the FT-IR analysis, mainly the peaks for PO_4^{3-} and OH^- groups in the hydroxyapatite can be identified in Fig. 2. Peaks at 560 – 610 and 1000 – 1100 cm^{-1} must be due to PO_4^{3-} . For the OH^- group the peak positions are 636 and 3572 cm^{-1} .

3.2. Effect of initial Sn^{2+} concentration and adsorbent dosage

The sorption of Sn^{2+} ions was carried out at different initial Sn^{2+} ion concentrations ranging from 80 to 140 mg/L, at pH 6.5, at 300 rpm with 120 min of contact time using nano-HAp. A rapid kinetic reaction of Sn removal by sorbent

occurred within the first 10 min (Fig. 3a). The aqueous Sn concentration at 10 min decreased to 42 , 62 , 80 and 98 mg/L by nano-HAp for 80 , 100 , 120 and 140 mg/L initial concentration respectively. Uptake of the Sn^{2+} also increased with increasing the initial metal concentration tending to saturation at higher metal concentrations. As shown in Fig. 3b, when the initial Sn^{2+} concentration increased from 80 to 140 mg/L, the uptake capacity of nano HAp increased from 1985 to 2400 mg/g. A higher initial concentration provides an important driving force to overcome all mass transfer resistances of the pollutant between the aqueous and solid phases, thus increasing the uptake (Aksu and Tezer, 2005).

The effect of nano-HAp dosage is presented in Fig. 4. It is evident that adsorption increases with the increase in the mass of sorbent and the uptake capacity of Sn^{2+} decreased from 2400 mg/g (34.28% removal) to 1233.33 mg/g (52.86% removal) with the increasing nano-HAp concentration from 0.01 to 0.03 g/L. This is because at the higher dosage of sorbent due to increased surface area, more adsorption sites are available causing higher removal of Sn^{2+} .

3.3. Effect of temperature

To study the effect of this parameter on the uptake of Sn^{2+} ions by nano-HAp, we selected the following temperatures: 25 , 45 and 65 °C. Fig. 5, illustrates the relationship between temperature and the amount of Sn^{2+} ions adsorbed onto nano-HAp at equilibrium time (120 min). As seen in Fig. 5, the adsorption of Sn^{2+} on nano-HAp increased from 2400 mg/g (34.28% removal) to 2750 mg/g (39.28% removal) when temperature was increased from 25 to 65 °C at an initial concentration of 140 mg/L. The increase in the equilibrium sorption of Sn^{2+} with temperature indicates that Sn^{2+} ions removal by adsorption on nano-HAp favors a high temperature. This may be a result of increase in the mobility of the Sn^{2+} ion with temperature. An increasing number of molecules may also acquire sufficient energy to undergo an interaction with active sites at the surface. Furthermore, increasing temperature may produce a swelling effect within the internal structure of nano-HAp enabling metal ions to penetrate further (Dogan and Alkan, 2003).

3.4. Determination of thermodynamic parameters

Thermodynamic parameters such as free energy change (ΔG°), and entropy change (ΔS°) can be estimated using equilibrium constants changing with temperature. The free energy change of the sorption reaction is given by the following equation:

$$\Delta G^\circ = -RTL \ln K_d \quad (3)$$

where ΔG° is the standard free energy change (J); R is the universal gas constant, 8.314 J/mol K and T is the absolute temperature (K). The distribution ratio (K_d) was calculated using Eq. (2):

$$K_d = \frac{\text{amount of metal in adsorbent}}{\text{amount of metal in solution}} = \frac{q_e}{C_e} \quad (4)$$

The distribution ratio (K_d) values increased with temperature, indicating the endothermic nature of adsorption. A plot of Gibbs free energy changes, ΔG° , versus temperature, T (K); was found to be linear. The values of ΔH° and ΔS° were determined from the slope and intercept of the plots according Eq. (5):

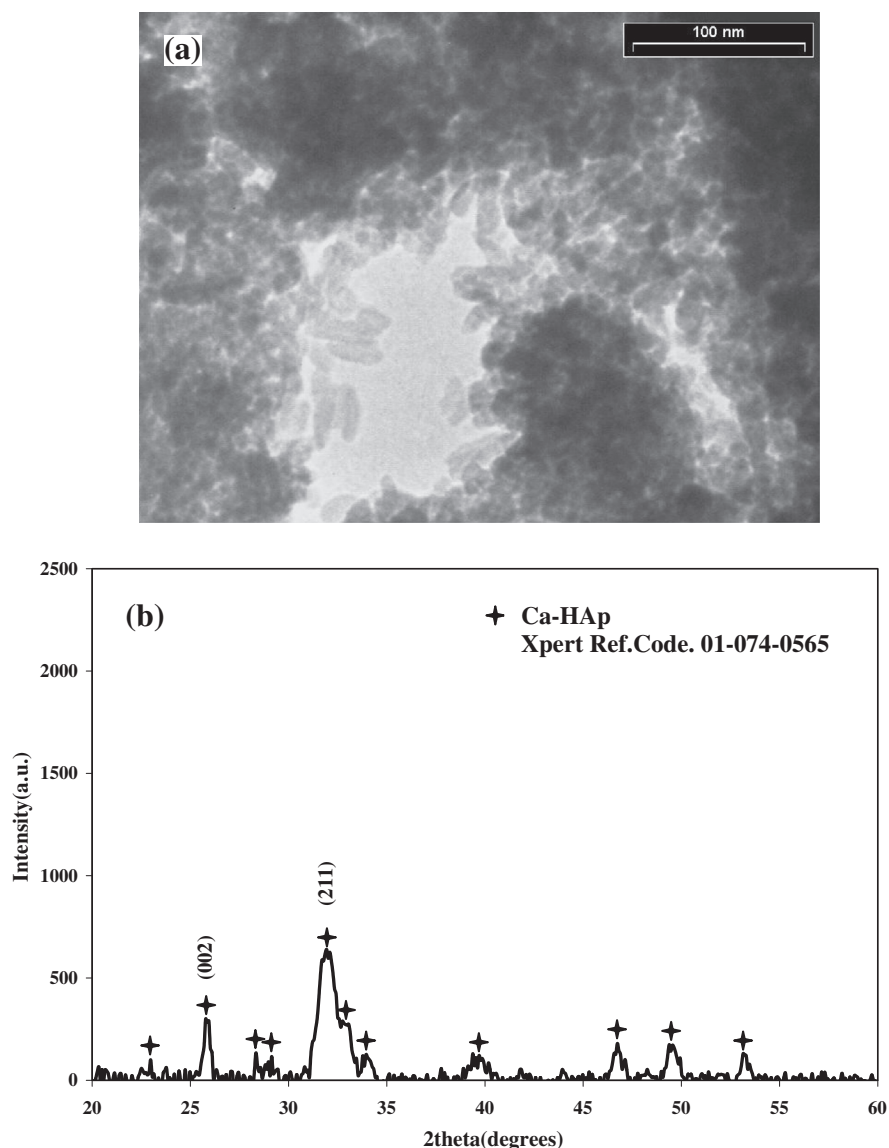


Figure 1 TEM micrograph (a) and XRD pattern (b) of calcium nanocrystalline hydroxyapatite after drying at 100 °C.

$$\Delta G^\circ = \Delta H^\circ - T\Delta S^\circ \quad (5)$$

The thermodynamic parameters Gibbs free energy change, ΔG° , are shown in Table 1. The enthalpy change, ΔH° , and the entropy change, ΔS° , for the sorption processes are calculated to be 4524 J/mol and 99.67 J/mol K, respectively. The negative values of ΔG° at various temperatures indicate the spontaneous nature of the adsorption process. The positive value of ΔS° indicates that there is an increase in the randomness in the system solid/solution interface during the adsorption process. In addition, the positive value of ΔH° indicates that the adsorption is endothermic. The positive value of ΔS° reflects the affinity of nano-HAp for Sn^{2+} ions and suggests some structural changes in tin and nano-HAp (Ho, 2003).

3.5. Adsorption isotherms

Analysis of the equilibrium data is important to develop an equation which accurately represents the results and which

could be used for design purposes (Aksu, 2002). Several isotherm equations have been used for the equilibrium modeling of adsorption systems.

The sorption data have been subjected to different sorption isotherms, namely, Langmuir, Freundlich, and Dubinin–Kaganer–Radushkevich.

The equilibrium data for metal cations over the concentration range from 80 to 140 mg/L at 25 °C have been correlated with the Langmuir isotherm (Langmuir, 1918):

$$\frac{C_e}{q_e} = \frac{1}{Q_0 K} + \frac{C_e}{Q_0} \quad (6)$$

where C_e is the equilibrium concentration of metal in the solution (mg/L), q_e is the amount adsorbed at equilibrium onto nano-HAp (mg/g), Q_0 and K are Langmuir constants related to sorption capacity and sorption energy, respectively. Maximum sorption capacity (Q_0) represents the monolayer coverage of the sorbent with the sorbate and K represents enthalpy of sorption and should vary with temperature. A lin-

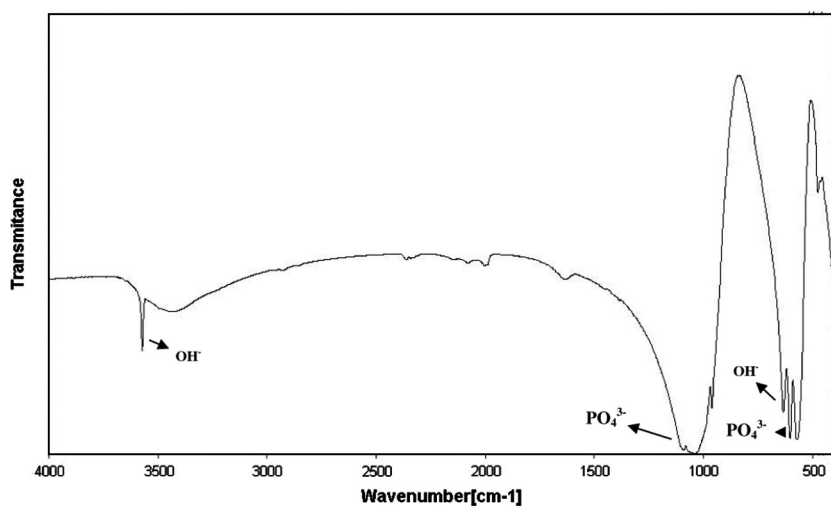


Figure 2 FTIR Spectroscopy analysis of the nano hydroxyapatite powder after drying at 100 °C.

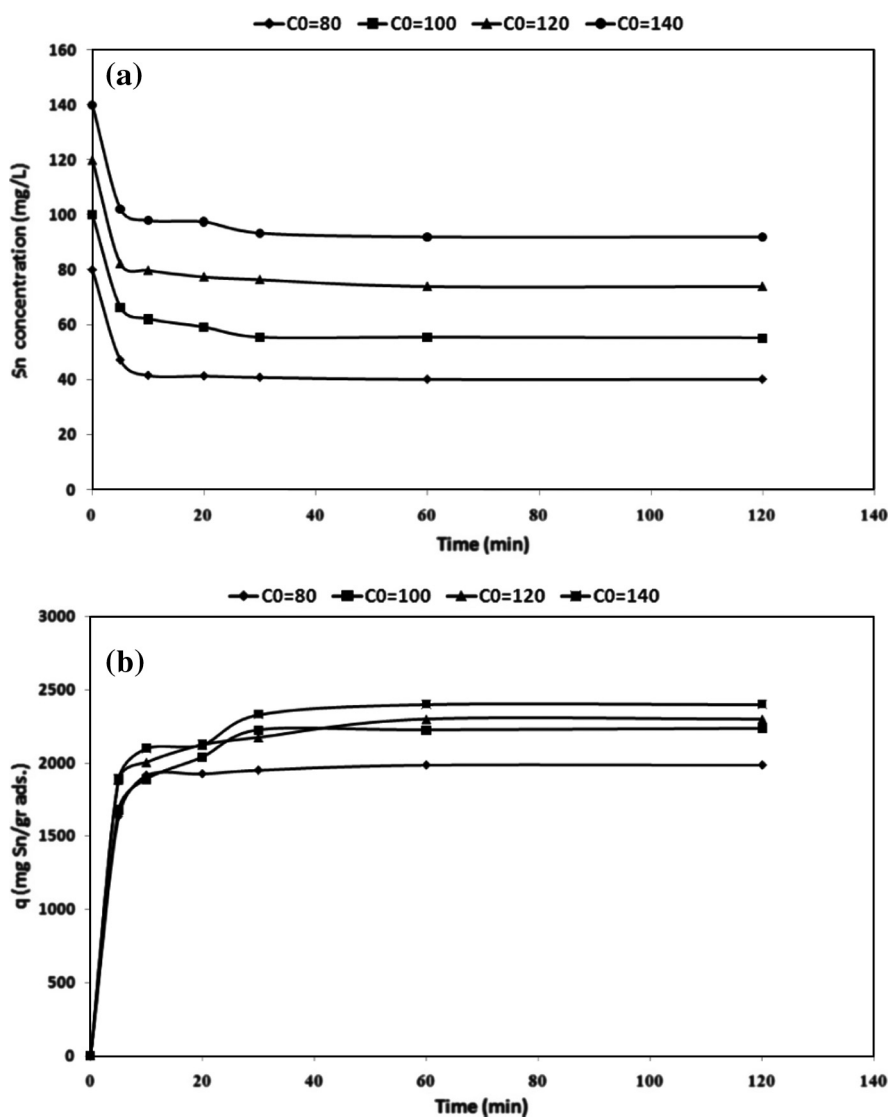


Figure 3 Time dependent concentration (a) and effect of initial concentration on removal of aqueous Sn²⁺ by nano hydroxyapatite sorbents (pH 6.5, adsorbent dosage = 0.01 g/L, 300 rpm agitating rate).

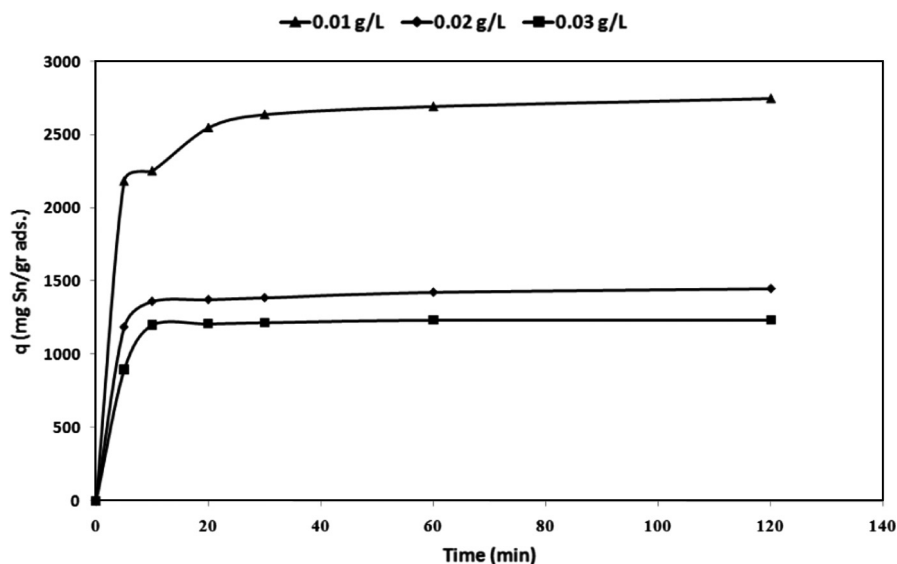


Figure 4 Effect of adsorbent dosage on removal of Sn^{2+} by nano hydroxyapatite (pH 6.5, initial metal concentration = 140 mg/L, 300 rpm agitating rate).

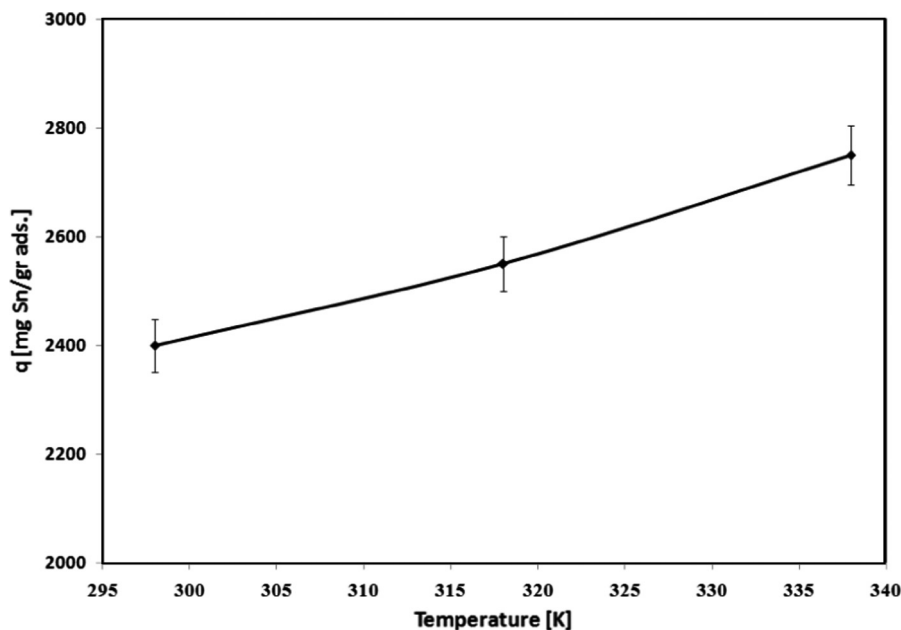


Figure 5 Uptake capacity of Sn^{2+} ions at different temperatures (pH 6.5, initial metal concentration = 140 mg/L, adsorbent dosage = 0.01 g/L, 300 rpm agitating rate).

ear plot is obtained when C_e/q_e is plotted against C_e over the entire concentration range of metal ions investigated.

The linearized Langmuir adsorption isotherms of Sn^{2+} ions are given in Fig. 6a. An adsorption isotherm is characterized by certain constants whose values express the surface properties and affinity of the sorbent and can also be used to find the sorption capacity of the sorbent.

The Freundlich sorption isotherm, one of the most widely used mathematical descriptions, usually fits the experimental data over a wide range of concentrations. This isotherm gives an expression encompassing the surface heterogeneity and the exponential distribution of active sites and their energies. The

Freundlich adsorption isotherms were also applied to the removal of Sn^{2+} on nano-HAp (Fig. 6b).

$$\ln q_e = \ln k_f + \frac{1}{n} \ln C_e \quad (7)$$

where q_e is the amount of metal ion sorbed at equilibrium per gram of adsorbent (mg/g), C_e the equilibrium concentration of metal ion in the solution (mg/L), k_f , and n the Freundlich model constants (Malkoc and Nuhoglu, 2003; Kadirvelu et al., 2001). Freundlich parameters, k_f and n , were determined by plotting $\ln q_e$ versus $\ln C_e$. The numerical value of $1/n < 1$ indicates that adsorption capacity is only slightly suppressed

Table 1 Thermodynamic parameters for the adsorption of Sn^{2+} onto nano hydroxyapatite.

T (K)	K_d	ΔG° (J/mol)	ΔH° (J/mol)	ΔS° (J/mol k)
298	26086.96	-25194.90		
318	28651.69	-27133.30	4524	99.67
338	32352.94	-2931.70		

at lower equilibrium concentrations. This isotherm does not predict any saturation of the sorbent by the sorbate; thus infinite surface coverage is predicted mathematically, indicating multilayer adsorption on the surface (Hasany et al., 2002).

The Dubinin–Kaganer–Radushkevich (D–K–R) equation has been used to describe the sorption of metal ions on clays. The D–K–R equation has the form:

$$\ln C_{\text{ads}} = \ln X_m - \beta \varepsilon^2 \quad (8)$$

where C_{ads} is the number of metal ions adsorbed per unit weight of adsorbent (mol/g), X_m (mol/g) is the maximum sorption capacity, β (mol^2/J^2) is the activity coefficient related to mean sorption energy, and ε is the Polanyi potential, which is equal to:

$$\varepsilon = RT \ln(1 + 1/C_e) \quad (9)$$

where R is the gas constant (kJ/mol K) and T is the temperature (K). The saturation limit X_m represents the total specific micropore volume of the sorbent. The sorption potential is independent of the temperature but varies according to the nature of the sorbent and the sorbate (Khan et al., 1995). The slope of the plot of $\ln C_{\text{ads}}$ versus ε gives β (mol^2/J^2) and the intercept yields the sorption capacity, X_m (mol/g). The sorption space in the vicinity of a solid surface is characterized by a series of equipotential surfaces having the same sorption potential. This sorption potential is independent of the temperature but varies according to the nature of the sorbent and the sorbate. The sorption energy can also be worked out using the following relationship:

$$E = 1/\sqrt{-2\beta}. \quad (10)$$

It is known that the magnitude of apparent adsorption energy E is useful for estimating the type of adsorption and if this value is below 8 kJ/mol the adsorption type can be explained by physical adsorption, between 8 and 16 kJ/mol the adsorption type can be explained by ion exchange, and over 16 kJ/mol the adsorption type can be explained by a stronger chemical adsorption than ion exchange; (Lin and Juang, 2002; Wang, 2004; Krishna et al., 2000). The plot of $\ln C_{\text{ads}}$ against ε^2 for metal ion sorption on nano-HAp is shown in Fig. 6c. The Langmuir, Freundlich and D–K–R adsorption constants from the isotherms and their correlation coefficients are also presented in Table 2.

The correlation factors R (0.997, 0.929 and 0.935 for Langmuir, Freundlich and D–K–R models, respectively) confirm good agreement between the two theoretical models and our experimental results. The maximum sorption capacity, Q_0 , calculated from the Langmuir equation is 2500 mg/g, while Langmuir constant K is 0.07 L/mg. The values obtained for Sn^{2+} from the Freundlich model showed a maximum adsorption capacity (K_f) of 899.64 mg/g with an affinity value (n) equal

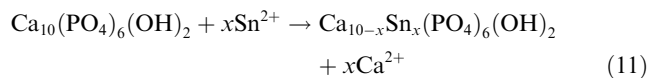
to 4.58. The values of sorption constants, derived from the D–K–R model are: 5092.06 mg/g (42.89 mmol/g) for X_m , $-2 \times 10^{-9} \text{ mol}^2/\text{J}^2$ for β and 15.81 kJ/mol for E .

The values indicate that the adsorption pattern for Sn^{2+} on nano-HAp followed the Langmuir isotherm ($R^2 > 0.997$), the D–K–R isotherm ($R^2 > 0.935$), and the Freundlich isotherm ($R^2 > 0.929$) at all experiments. It is clear that the Langmuir isotherm is the best fit for the sorption of Sn^{2+} on nano-HAp. When the system is in a state of equilibrium, the distribution of Sn^{2+} between nano HAp and the Sn^{2+} solution is of fundamental importance in determining the maximum sorption capacity of nano HAp for the Sn^{2+} ion from the isotherm. The E values are 15.81 kJ/mol for Sn^{2+} , on the nano HAp. It is the orders of an ion-exchange mechanism, in which the sorption energy lies within 8–16 kJ/mol.

Generally, HAp selectivity toward divalent metal cations is a result of the ion-exchange process with Ca^{2+} ions (Monteil Rivera and Fedoroff, 2002). Ionic radius of Sn^{2+} (0.71 Å) slightly differ from that of Ca^{2+} (0.99 Å), and it can substitute Ca^{2+} in the HAp crystal lattice. Fig. 7 presents the XRD patterns of the Sn^{2+} -loaded sample. No structural changes of nano HAp were detected by the powder X-ray diffraction analysis of the solid residue with the maximum amount of uptake capacity of Sn^{2+} , obtained after interaction of 0.01 g/L of nano HAp with 140 mg/L Sn^{2+} solution, at pH 6.5, at 300 rpm with 120 min of contact time. The sample was indexed in the hexagonal system with space group $P6_3/m$. The diffractogram's evidence clarifies that all XRD peaks were shifted toward upper diffraction angles for Sn-HAp particles (maximum peak: from $2\theta = 31.94^\circ$ to $2\theta = 32.11^\circ$). These shifts are indicative of the decrease in unit cell dimensions which is due to the replacement of Sn^{2+} (ionic radius 0.71 Å), which is smaller than Ca^{2+} (ionic radius 0.99 Å), into the crystal lattice of apatite molecules.

The reaction mechanism corresponds to the equimolar exchange of tin and calcium yielding $\text{Ca}_{10-x}\text{Sn}_x(\text{PO}_4)_6(\text{OH})_2$, where x can vary from 0 to 10 depending on the reaction time and experimental conditions. Our results of synthesized nano-HAp agreed with those described elsewhere that the proposed mechanism for Sn^{2+} removal by HAp comprises two steps: firstly, rapid surface complexation of Sn^{2+} on the $\equiv\text{POH}$ sites of HAp which causes the decrease of the pH (from pH = 6.5 to pH = 6.0 for initial metal concentration = 140 mg/L, dosage = 0.01 g/L, 300 rpm agitating rate) and secondly, partial dissolution of calcium followed by the precipitation of an apatite with formula: $\text{Sn}_x\text{Ca}_{10-x}(\text{PO}_4)_6(\text{OH})_2$.

In which Sn^{2+} ions are first adsorbed on the nano HAp surface and substitution with Ca^{2+} ion occurs as described by the following equation:



3.6. Sorption kinetics

Sorption kinetic studies were carried out in order to understand the behavior of nano-HAp toward Sn^{2+} metal. The sorption kinetics includes two phases: a rapid metal sorption stage followed by a much slower stage before the equilibrium was established. It was found that the mass transfer was the

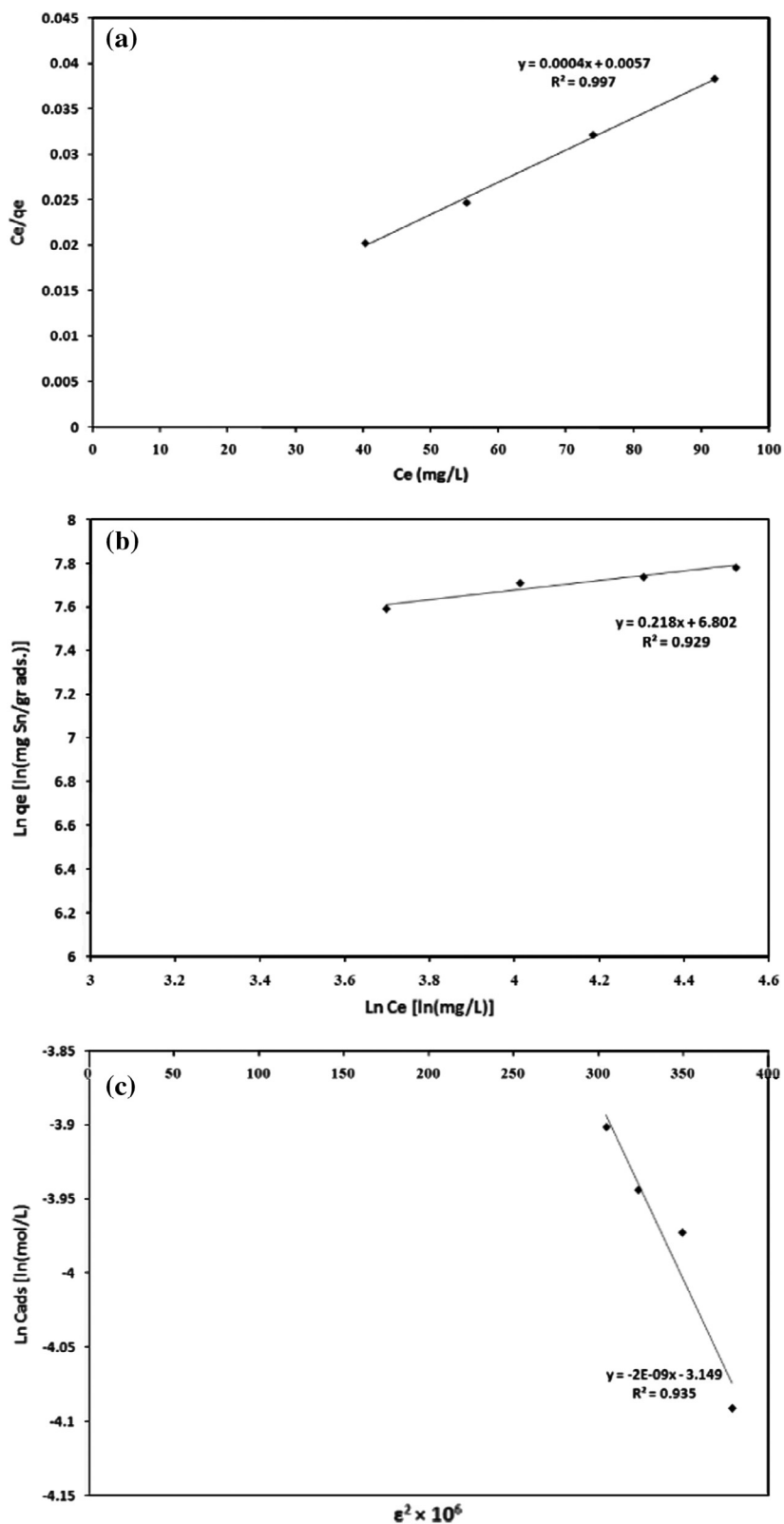


Figure 6 Linear fits of experimental data obtained using Langmuir (a), Freundlich (b) and D-K-R (c) sorption isotherms for the adsorption of Sn^{2+} onto nano Hydroxyapatite (pH 6.5, initial metal concentration = 80, 100, 120 and 140 mg/L, adsorbent dosage = 0.01 gr/L, 300 rpm agitating rate).

Table 2 Langmuir, Freundlich and D-K-R constants for adsorption of Sn²⁺ onto nano hydroxyapatite.

Langmuir adsorption isotherm constants		
Q_o (mg/g)	K (L/mg)	R^2
2500	0.07	0.997
Freundlich adsorption isotherm constants		
k_f (mg/g)	n	R^2
899.64	4.58	0.929
DKR adsorption isotherm constants		
X_m (mg/g)	β (mol ² /J ²)	R^2
5092.06	-2×10^{-9}	0.935

key factor in the metal sorption (Chen and Wang, 2004). The sorption kinetics describes the metal sorption rate, which in turn governs the residence time of the sorption reaction and also the efficiency of the sorption process. Out of the several kinetic models available to examine the controlling mechanism of the sorption kinetic process and to test the experimental data, the Lagrangian equation or pseudo-first-order equation and pseudo-second-order equation have been used for the metal sorption kinetics of nano-HAp.

The linearized form of the pseudo-first-order equation:

$$\log(q_e - q) = \log q_{e \text{ cal}} - \frac{k_1}{2.303} t \quad (12)$$

where q_e is the metal sorbed at equilibrium (mg g⁻¹), q is the amount of the metal adsorbed (mg g⁻¹) at any time t , k_1 is the first-order rate constant. The first-order rate constant k_1 and q were determined from the slopes and intercept of plots of $\log(q_e - q)$ vs t at different metal concentration.

The linearized form of the pseudo-second-order equation for the kinetics of absorption described by Ho and Chiang (2001) is as follows:

$$\frac{t}{qt} = \frac{1}{k_2 q_{e \text{ cal}}^2} + \frac{1}{q_{e \text{ cal}}} \quad (13)$$

The second-order rate constant (k_2) and $q_{e \text{ cal}}$ were determined from the slope and intercept of the plot obtained by plotting t/qt vs t .

Linear plots of $\log(q_e - q_t)$ versus t and t/qt versus t are depicted in Fig. 8a and Fig. 8b at 25, 45 and 65 C, respectively. A comparison of the results with the correlation coefficients is shown in Table 3. The pseudo-second-order kinetic model obtained for Sn²⁺ sorption at various temperatures showed a better correlation of the result than the pseudo-first-order equation model. The correlation coefficients for the second order kinetic model obtained at 140 ppm concentrations at different temperatures were high. The values of k_2 at 25, 45 and 65 C were varied from 0.00023 to 0.000191 min⁻¹. The higher rate of metal sorption in the beginning (Fig. 3b) could be due to the presence of the active site in the nano-HAp surface, available for the sorption of metals. Once the sorptive sites are exhausted, the uptake rate may be controlled by the rate of intra particle diffusion. The activation energy E_a was determined using the Arrhenius equation (Aksu, 2002):

$$\text{Ln}K_{ad} = \text{Ln}A - \frac{E_a}{RT} \quad (14)$$

where k_{ad} (k_2) is the rate constant value for the metal adsorption, E_a the activation energy in kJ mol⁻¹, T the temperature in Kelvin, and R is the gas constant ($= 8.314 \text{ kJ mol}^{-1} \text{ K}^{-1}$). When $\text{Ln}k_{ad}$ is plotted versus $1/T$, a straight line with slope $-E_a/R$ is obtained. The activation energy for the adsorption system of Sn²⁺ onto nano-HAp was found as 4.125 kJ mol⁻¹ from the slope of this plot, indicating the physical adsorption. As known when the rate is controlled by intra-particle diffusion mechanism, the activation energy is low and hence it can be concluded that the process is controlled by intra-parti-

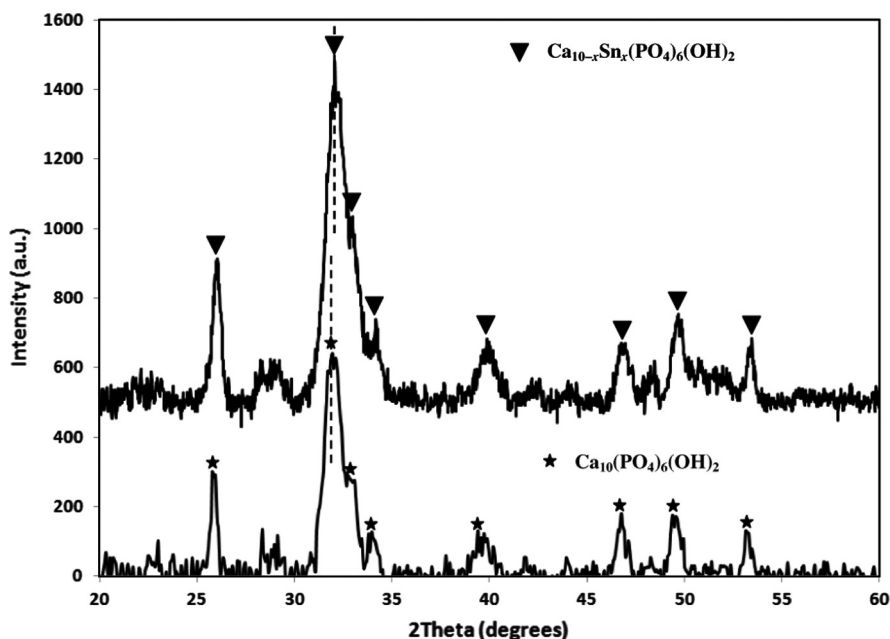


Figure 7 XRD pattern of the solid residue with maximum amount of uptake capacity of Sn²⁺ (pH 6.5, initial metal concentration = 140 mg/L, adsorbent dosage = 0.01 g/L, 300 rpm agitating rate).

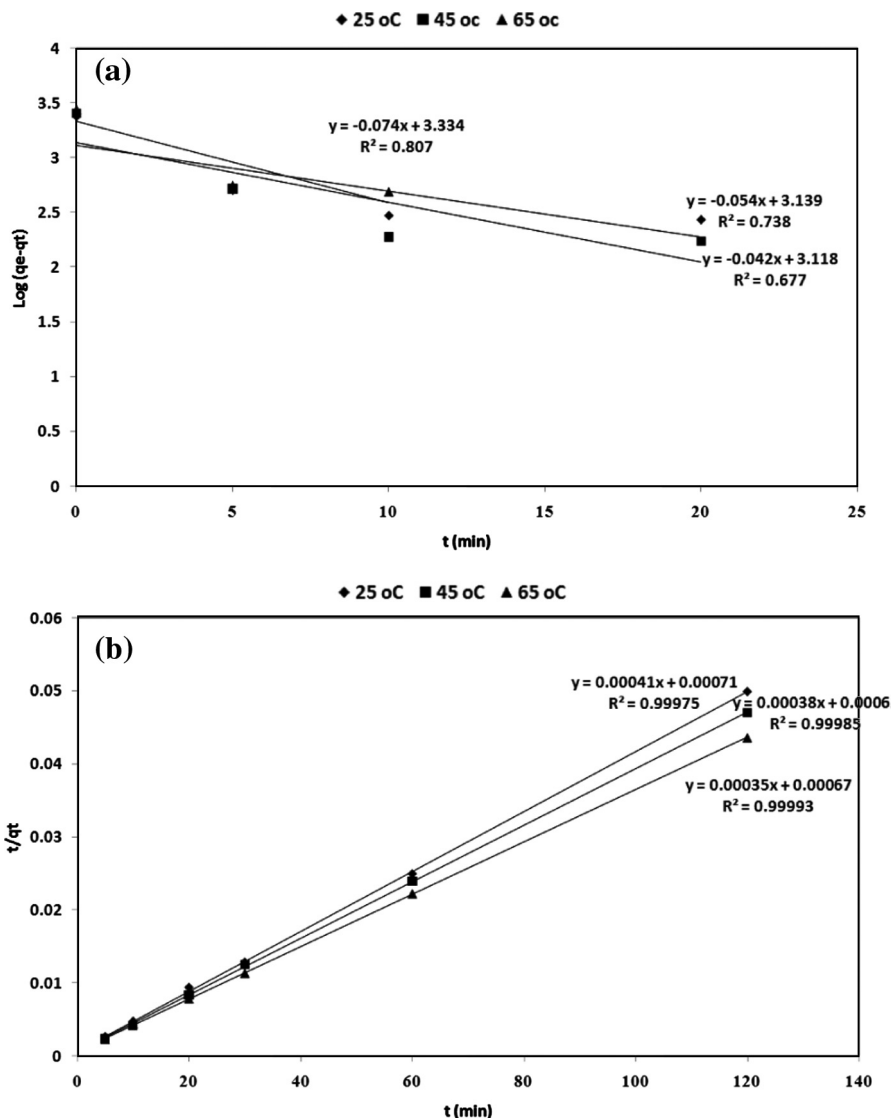


Figure 8 Linear fit of experimental data obtained using pseudo-first order kinetic model (a) and pseudo-second order kinetic model (b) (pH 6.5, initial metal concentration = 140 mg/L, adsorbent dosage = 0.01gr/L, 300 rpm agitating rate).

Table 3 A comparison of the first and second order kinetic rate constants and calculated $q_{e\text{ cal}}$ values obtained at different temperatures (pH 6.5, initial metal concentration = 140 mg/L, adsorbent dosage = 0.01gr/L, 300 rpm agitating rate).

T [°C]	K_1 [min ⁻¹]	$q_{e\text{ cal}}$ [mg/g]	R^2
<i>Pseudo-first-order kinetic model</i>			
25	0.09672	1312.20	0.67761
45	0.12436	1377.21	0.73865
65	0.17042	2157.74	0.80748
<i>Pseudo-second-order kinetic model</i>			
25	0.00023	2440.45	0.99975
45	0.00024	2577.78	0.99985
65	0.00019	2790.49	0.99993

4. Conclusions

The present investigation shows that nano HAp is an effective adsorbent for the removal of Sn²⁺ from aqueous Sn²⁺ solutions. The adsorption process is a function of the adsorbent dosage, the initial Sn²⁺ concentration and the temperature. The efficiency of Sn²⁺ adsorption increased with an increase in the adsorbent dosage. Isotherm studies indicate that the Langmuir model fits the experimental data better than Freundlich and D–K–R models. The adsorption equilibrium was described well by the Langmuir isotherm model with a maximum adsorption capacity of 2500 mg/g of Sn²⁺ ions on nano HAp. The results of XRD analysis strongly support the ion-exchange as a main mechanism for Sn²⁺ removal by nano HAp. The results show that the Sn²⁺ uptake by nano hydroxyapatite proceeds with a rapid surface complexation of the Sn²⁺ on the ≡POH site before the formation of a compound of formula Ca_{10-x}Sn_x(PO₄)₆(OH)₂. Thermodynamic calculations showed that the Sn²⁺ sorption process of nano

cle diffusion, which is a physical step in the adsorption process (Dogan and Alkan, 2003).

HAp has an endothermic and spontaneous nature. The kinetic behavior of the metal toward nano-HAp demonstrated pseudo-second-order kinetics rather than pseudo-first-order kinetics. The second order kinetic model was successfully applied to the experimental data, confirming that adsorption was controlled by intra-particle diffusion.

Acknowledgment

This research was supported by the Research Project Unit at the Maybod Branch, Islamic Azad University, Maybod, Iran under the Project No. P/870358.

References

- Aksu, Z., 2002. Determination of the equilibrium, kinetic and thermodynamic parameters of the batch biosorption of nickel(II) ions onto *Chlorella vulgaris*. *Process Biochem.* 38, 89–99.
- Aksu, Z., Tezer, S., 2005. Biosorption of reactive dyes on the green alga *Chlorella vulgaris*. *Process Biochem.* 40, 1347–1361.
- Aksu, Z., Tunc, O., 2005. Application of biosorption for penicillin G removal: comparison with activated carbon. *Process Biochem.* 40, 831–847.
- Chen, J.P., Wang, L., 2004. Characterization of metal adsorption kinetic properties in batch and fixed bed reactors. *Chemosphere* 54, 397–404.
- Chen, X., Wright, J.W., Conca, J.L., Peurrung, L.M., 1997. Effects of pH on heavy metal sorption on mineral apatite. *Environ. Sci. Technol.* 31 (3), 624–631.
- Czerniczyniec, M., Farias, S., Magallanes, J., Cicerone, D. 2003. Arsenic adsorption on biogenic HAP: Solution composition effects. In: 11th International Conference on Surface and Colloid Science, Fozdo Iguazu, Brazil, 269.
- Dogan, M., Alkan, M., 2003. Adsorption kinetics of methyl violet onto perlite. *Chemosphere* 50, 517–528.
- Elliott, J.C., 1994. *Structure and Chemistry of the Apatites and Other Calcium Orthophosphates*. Elsevier, Amsterdam.
- Fuller, C., Bargar, J., Davis, J., Piana, M., 2002. Mechanisms of uranium interactions with hydroxyapatite: implications for groundwater remediation. *Environ. Sci. Technol.* 36 (2), 158–165.
- Hasany, S.M., Saeed, M.M., Ahmed, M., Radioanal, J., 2002. Sorption and thermodynamic behavior of zinc(II)-thiocyanate complexes onto polyurethane foam from acidic solutions. *Nucl. Chem.* 252 (3), 477–484.
- Ho, Y.S., 2003. Removal of copper ions from aqueous solution by tree fern. *Water Res.* 37, 2323–2330.
- Ho, Y., Chiang, C., 2001. Sorption studies of acid dye by mixed sorbents. *Adsorption* 7, 139–147.
- Kadirvelu, K., Thamaraiselvi, K., Namasivayam, C., 2001. Adsorption of nickel(II) from aqueous solution onto activated carbon prepared from coirpith. *Sep. Purif. Technol.* 24, 497–505.
- Khan, S.A., Rehman, U.R., Khan, M.A., 1995. Adsorption of chromium(III), chromium(VI) and silver(I) on bentonite. *Waste Manage.* 15 (4), 271–282.
- Krestou, A., Xenidis, A., Pnias, D., 2004. Mechanism of aqueous uranium(VI) uptake by a natural zeolitic tuff. *Miner. Eng.* 16 (12), 1363–1370.
- Krishna, B.S., Murty, D.S.R., Prakash, B.S.J., 2000. Thermodynamics of chromium(VI) anionic species sorption onto surfactant-modified montmorillonite clay. *J. Colloid Interface Sci.* 229 (1), 230–236.
- Langmuir, I., 1918. The adsorption of gases on plane surfaces of glass, mica and platinum. *J. Am. Chem. Soc.* 40 (9), 1361–1403.
- Laperche, V., Traina, S.J., Gaddam, P., Logan, T.J., Ryan, J.A., 1996. Chemical and mineralogical characterizations of Pb in a contaminated soil: reactions with synthetic apatite. *Environ. Sci. Technol.* 30, 3321–3326.
- Leyva, A., Marrero, J., Smichowski, P., Cicerone, D., 2001. Sorption of antimony onto hydroxyapatite. *Environ. Sci. Technol.* 35 (18), 3669–3675.
- Lin, S.H., Juang, R.S., 2002. Heavy metal removal from water by sorption using surfactant-modified montmorillonite. *J. Hazard. Mater. B* 92 (3), 315–326.
- Ma, Q.Y., Traina, S.J., Logan, T.J., Ryan, J.A., 1993. In situ lead immobilization by apatite. *Environ. Sci. Technol.* 27, 1803–1810.
- Ma, Q.Y., Traina, S.J., Logan, T.J., Ryan, J.A., 1994. Effects of Aqueous Al, Cd, Cu, Fe(II), Ni, and Zn on Pb immobilization by hydroxyapatite. *Environ. Sci. Technol.* 28, 1219–1228.
- Malkoc, E., Nuhoglu, Y., 2003. The removal of chromium(VI) from synthetic wastewater by *Ulothrix zonata*. *Fres. Environ. Bull.* 12 (4), 376–381.
- Mavropoulos, E., 2002. Studies on the mechanisms of lead immobilization by hydroxyapatite. *Environ. Sci. Technol.* 36, 1625–1629.
- McGrellis, S., Serafini, J., Jean, J., Pastol, J., Fedoroff, M., 2001. Influence of the sorption protocol on the uptake of Cd ions in calcium hydroxyapatite. *Sep. Purif. Technol.* 24, 129–138.
- Mobasherpour, I., Soulati Heshajin, M., Kazemzadeh, A., Zakeri, M., 2007. Synthesis of nanocrystalline hydroxyapatite by using precipitation method. *Jalcom* 430, 330–333.
- Mobasherpour, I., Salahi, E., Pazouki, M., 2011. Removal of divalent cadmium cations by means of synthetic nano crystallite hydroxyapatite. *Desalination* 266, 142–148.
- Monteil Rivera, F., Fedoroff, M., 2002. Sorption of inorganic species on apatites from aqueous solutions. In: *Encyclopedia of Surface and Colloid Science*. Marcel Dekker Inc., New York.
- Nzihou, A., Sharrock, P., 2002. Calcium phosphate stabilization of fly ash with chloride extraction. *Waste Manag.* 2002, 235–239.
- Reichert, J., Binner, J., 1996. An evaluation of hydroxyapatite-based filters for removal of heavy metal ions from aqueous solutions. *J. Mater. Sci.* 31 (5), 1231–1241.
- Takeuchi, Y., Arai, H., 1990. Removal of coexisting Pb^{2+} , Cu^{2+} , Cd^{2+} ions from water by addition of hydroxyapatite powder. *J. Chem. Eng. Jpn.* 23, 75–80.
- Tanaka, H., Futaoka, M., Hino, R., Kandori, K., Ishikawa, T., 2005. Structure of synthetic calcium hydroxyapatite particles modified with pyrophosphoric acid. *J. Colloid Interface Sci.* 283 (2), 609–612.
- Vega, E.D., Pedregosa, J.C., Narda, G.E., 1999. Interaction of oxovanadium(IV) with crystalline calcium hydroxyapatite: surface mechanism with no structural modification. *J. Phys. Chem. Solids* 60 (6), 759–766.
- Wang, C.C., 2004. Effects of exchanged surfactant cations on the pore structure and adsorption characteristics of montmorillonite. *J. Colloid Interface Sci.* 280 (1), 27–35.
- Wasewar, K.L., Kumar, S., Prasad, B., 2009. Adsorption of tin using granular activated carbon. *J. Environ. Pro. Sci.* 3, 41–52.